ELSEVIER

Journal of Nuclear Materials 305 (2002) 224–231

journal of nuclear materials

www.elsevier.com/locate/jnucmat

Letter to the Editors

Studies of second phase particles in different zirconium alloys using extractive carbon replica and an electrolytic anodic dissolution procedure

Caroline Toffolon-Masclet [a,*], Jean-Christophe Brachet [a], Gilles Jago [b]

[a] *DMN/SRMA, CEA Saclay, 91191 Gif-sur-Yvette cedex, France*

[b] *Hutchinson Corporate Research Center, rue Gustave Nourry, BP 31, 45120 Chalette sur Loing, France*

Received 1 February 2002; accepted 17 June 2002

Abstract

Zirconium alloys are widely studied for applications as cladding tubes and structural components of PWR fuel assemblies. Due to their influence on some of the alloys properties (corrosion resistance, irradiation growth, ...), the crystallographic structure and the chemical stoichiometry of the second phase particles (SPP) precipitated in these alloys have to be well established. The aim of this paper is to present the results obtained using two methods of SPP extractions. The first one, the extractive carbon replica method, allowed us to determine the chemical composition of SPP in different zirconium alloys: Zr–Sn–Fe–Cr (Zircaloy-4®), Zr–Sn–Fe–Cr–(V,Mo), Zr–Nb and Zr–Nb–Fe alloys. The second one, an anodic dissolution procedure of the matrix, is an interesting way of isolating SPP from the surrounding α-Zr matrix, giving access to a precise determination of the crystallographic structure and lattice parameters of the SPP by X-ray diffraction. This procedure was validated for Zy-4 by comparing the SPP size distribution obtained by extraction with that directly measured on a massive Zy-4 alloy (i.e. the SPP size distributions were the same for both measurements).

1. Introduction

Zirconium alloys are extensively used in nuclear power reactor fuel elements (fuel cladding and structural materials). The will to extend fuel cladding material life times in nuclear reactors has prompted the development of new zirconium alloys with improved resistance to long-term corrosion, and to irradiation growth and adequate mechanical properties. In that context, zirconium alloys with addition of various elements (Nb, Fe, V, Mo) were studied. The fuel cladding in-reactor behavior closely depends upon the microstructure and chemistry of the alloys. Especially, the effect of second phase particles (SPP) on metallurgical properties and corrosion has to be taken into account [1–5]. Thus, a thorough knowledge of the crystallography, chemical composition and size distribution of these SPP is essential.

Due to the small volume fraction and sizes of these SPP, their study by scanning electron microscopy (SEM) on massive alloys or by transmission electron microscopy (TEM) on thin foils, by microanalysis (energy dispersive X-ray spectroscopy – EDS) and using electron diffraction, is quite difficult due to the matrix contribution on the EDS analysis spectrum and on the electron diffraction patterns. Thus, the use of SPP extraction methods is of great interest. Previously, Yang et al. [6] have already developed a method of electrochemic extraction of SPP, but limited their study to the extraction of SPP in Zy-4 alloys.

The aim of the present study was to develop a method (anodic dissolution) which allows the extraction

* Corresponding author. Tel.: +33-1 69 08 21 39; fax: +33-1 69 08 71 30.

E-mail address: toffolon@cea.fr (C. Toffolon-Masclet).

0022-3115/02/$ - see front matter © 2002 Elsevier Science B.V. All rights reserved.
PII: S0022-3115(02)00911-X

of all kinds of SPP, stable or metastable, which can be found in the different Zr alloys, that is: Zy-4, Zr–Nb–(Fe,Sn), and Zr–Sn–Fe–Cr–(V,Mo) alloys [7]. The extracted residue (powder form) is characterized by X-ray diffraction in order to determine crystallographic data.

A second method, the carbon replica, was also applied in order to determine the chemical composition of the SPP (using TEM) and to valid the anodic dissolution method. This article briefly describes the experimental procedures developed and the results obtained on several zirconium alloys.

2. Experimental procedure

2.1. Materials

The alloys were supplied by Framatome-ANP/Zircotube company for Zircaloy-4, Framatome-ANP/Cezus company for Zr–1%Nb and ZrNbFe alloys, and Teledyne Wah Chang company for Zr–2.5%Nb. Also, some experimental Zr–Sn–Fe–Cr–(V,Mo) alloys were elaborated by CEA (Letram), by arc-melting and then hot and cold rolled down to sheets of ~1 mm thick. The chemical compositions of these alloys are listed in Table 1.

The materials supplied by CEA (alloys 3, 4, 7 and 9) were melted into 300 g ingots by non-consumable arc-melting. Four melting cycles were performed in order to ensure a good chemical homogeneity. The ingots were transformed to about 1 mm-thick plates by means of a standard zirconium alloy manufacturing process consisting of beta quench from 1100 °C, alpha hot rolling at 700 °C and several cold rolling with intermediate annealing at 700 °C. These fabrication sequences lead to a fully recrystallized state.

Cezus as-received materials (alloys 1, 2, 5 and 6) were standard fully α-recrystallized industrial pressure tube shape except alloy 6, which corresponds to a 1 mm diameter extruded bar.

The Wah-Chang as-received material (alloy 8) corresponds to a 2 mm-thick plate hot rolled and recrystallised in the $\alpha + \beta$ domain.

Alloys 10–13 were obtained by arc-melting. From all melts, sheets were manufactured applying a manufacturing sequence of forging, β-quench, and hot and cold rolling with intermediate annealing in the α-temperature range (<600 °C). A final annealing of several hours was performed in order to obtain a fully α-recrystallized structure.

2.2. Experimental procedures

2.2.1. Carbon extraction replica

The carbon replica technique yields measurements of SPP chemical compositions without matrix contribution. This technique consists of a single-stage carbon extraction. A carbon layer is sputtered on the specimen surface and then, an electro-etching procedure is performed in order to collect the replicas.

The determination of SPP stoichiometries was performed using a scanning energy dispersive device (STEM/X-EDS). The carbon replica technique allows the determination of particle chemical composition as small as a few ten nanometers.

Table 1
Chemical composition of the different Zr-alloys studied

Alloy	Main alloying elements (wt%)						Main impurity contents (weight ppm)		
	Sn	Fe	Mo	V	Nb	Cr	O	N	Cu
1 (Zy-4)	1.3	0.20	/	/	/	0.1	1200	18	<50
2	0.6	0.60	/	0.4	/	0.1	1200	15	<50
3	1.2	0.60	/	0.33	/	0.1	1600	650	100[a]
4	1.25	0.55	0.56	/	/	0.1	1580	26	2600[a]
5 (Zr–1Nb)	/	0.05	/	/	1.07		970	23	<10
6	/	0.02	/	/	1.03		1140	25	<10
7	1.00	0.4	/	/	0.95		1200	15	<50
8 (Zr–2.5Nb)	/	0.07	/	/	2.60		1000	28	<25
9	3.15	0.03	1.00	/	1.00		~1200	20	<50
10 (Zr–Nb–Fe)	0.5	0.4	/	/	1.10		1200	/	/
11	/	0.75	/	/	1.00		1200	/	/
12	/	0.45	/	/	2.00		1200	/	/
13	/	0.75	/	/	2.00		1200	/	/

[a] N pollution during the elaboration of this experimental alloy by arc-melting.

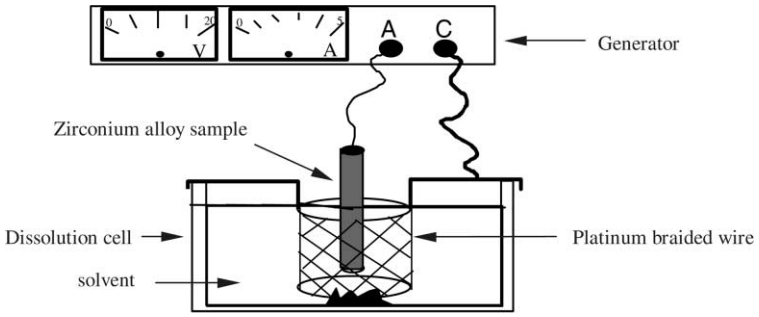

Fig. 1. Scheme of the electro-etching system for SPP extraction by electrolytic anodic dissolution of the matrix (for more details, see [7]).

2.2.2. Electro-etching extraction procedure

A scheme of the electro-etching system is presented in Fig. 1. The electrolyte composition is methanol: 40–90 vol.%, 2-Butoxyethanol: 0–20 vol.% and perchloric acid: 10–40 vol.%. The operating intensity is ranging from 2.5 to 4.5 A at room temperature [7].

The powder residue obtained after dissolution of the Zr matrix and centrifugation of the electrolyte was analyzed by X-ray diffraction, using a Siemens X-ray diffractometer (Cu anticathode).

3. Results and discussion

3.1. Composition of SPP

STEM/X-EDS measurements on carbon replica performed on more than 20 particles per sample enabled us to determine the stoichiometries of the SPP of the different alloys studied (Table 2). Most of the intermetallic phases observed in these alloys are Laves phase types $Zr(X_1,X_2)_2$, where X_1 and X_2 can be: Fe, Cr, V, Nb, Mo and/or Cu.

3.1.1. Zr–Sn–Fe–Cr alloys

In Zircaloy-4 alloy (alloy 1), one can observe the well-known $Zr(Fe_{1-x},Cr_x)_2$ type precipitates, with $x = 0.4$, and a Fe/Cr ratio close to 1.5. These results are in good agreement with those from Svechnikov et al. [8] and Versaci and Ipohorski [9] in Zircaloy-4 alloys.

3.1.2. Zr–Sn–Fe–Cr–V alloys

In alloys 2 and 3, we find an intermetallic phase with a Laves phase type $Zr(Fe_{1-x}V_x)_2$ where $x \approx 0.35$, which is smaller than some of the values found in the literature [10,11]. The value corresponds to a Fe/V ratio close to the Fe/Cr one of the Laves phases in Zircaloy-4 alloy.

Some $(Fe_x(V+Cr)_{1-x})Zr_{\sim 2.5}$ phases are also observed, with a $Fe/(V+Cr)$ ratio close to 1.85. A similar type of stoichiometry has already been mentioned by Arias et al. [12] in Zircaloy-2 alloys: $Zr_2(Fe_{0.6}Ni_{0.4})$ (Fe/Ni ratio equal to 1.5).

Table 2
SPP stoichiometries determined by STEM/X-EDS measurements on carbon extraction replicas

Alloy	SPP mean composition (at.%) and/or phase type
1 (Zy-4)	$Zr(Fe_{0.58},Cr_{0.42})_2$
2	$(Fe_{0.65}, V_{0.22}Cr_{0.13})Zr_{2,5}$ (minor)
	$Zr(Fe_{0.58}V_{0.37}Cr_{0.05})_2$
3	$Zr(Fe_{0.66}V_{0.33})_2$
4	β-Zr (Mo ∼ 10%)
	$Zr(Fe_{0.35}, Mo_{0.65})_2$ (minor)
	$Zr(Fe, Cr, Cu)_2$ (minor)
5 (Zr–1Nb)	β-Nb (Nb ∼ 80%)
6	β-Zr (Nb ∼ 15–20%)
7	β-Zr (Nb ∼ 15–20%)
	$Zr_{52}Fe_{36}Nb_{12}$
8 (Zr–2.5 Nb)	β-Nb (Nb ∼ 80%)
9	β-Zr (Nb ∼ 15–20%)
10 (Zr–Nb–Fe)	$Zr_{60}Nb_{10}Fe_{30}$
	$Zr_{35}Nb_{35}Fe_{30}$
11	$Zr_{60}Nb_{10}Fe_{30}$
12	$Zr_{35}Nb_{35}Fe_{30}$
	β-Nb (Nb ∼ 80%)
13	$Zr_{35}Nb_{35}Fe_{30}$
	$Zr_{60}Nb_{10}Fe_{30}$ (minor)

3.1.3. Zr–Sn–Fe–Cr–Mo alloys

The SPP present in alloy 4 are Laves phases with the following chemical composition: $Zr(Fe_{0.35}Mo_{0.65})_2$ ($x = 0.65$). The Fe/Mo ratio (0.54) is close to the Fe/Cr ratio obtained by [9] on Zy-2.

3.1.4. Zr–Nb and Zr–Nb–Fe systems

In alloys 10, 12 and 13, an intermetallic phase, with a HC structure, which stoichiometry is close to that of a

Laves phase, is present: 35Zr–35Nb–30Fe (at.%) [13]. This phase is also detected in Zr–1Nb–1.2Sn–0.35Fe (E635 alloy) as mentioned by Nikulina et al. [14]. These authors give a range of stoichiometry for this intermetallic phase: (36–43)Zr–(35–45)Nb–(20–30)Fe (at.%). A more accurate composition of this phase is given by Shishov et al. [15] who studied more recently a Zr–1.25%Sn–1%Nb–0.15%Fe alloy: 34Zr–40Nb–26Fe (at.%). The chemical compositions of the phases mentioned in the literature are in good agreement with our own results.

A second intermetallic phase, with a FCC structure, is encountered in ZrNbFe alloys, specifically in alloys 10, 11 and 13, which corresponds to a 60Zr–10Nb–30Fe (at.%) chemical composition [13]. A similar phase is mentioned by Petkov and Cherkashin in [16], for which they determined the following stoichiometry: $Zr_{50}Nb_{10}Fe_{40}$.

This phase was also observed in E635 alloy by Shishov et al. [15]. The following composition is given: 60Zr–11Nb–29Fe (at.%), which is very close to our own results.

It is of interest to mention the β-stabilising effect of molybdenum and niobium in Zr alloys. When Zr–Nb–Fe and Zr–Sn–Fe–Cr–Mo alloys are thermally treated in the lower $\alpha + \beta$ temperature range (600–750 °C), the high-temperature metastable β-Zr phase enriched with Nb or Mo is retained at room temperature. One can make the assumption that this is related to the very slow diffusion rates of Mo and Nb preventing the decomposition of Nb

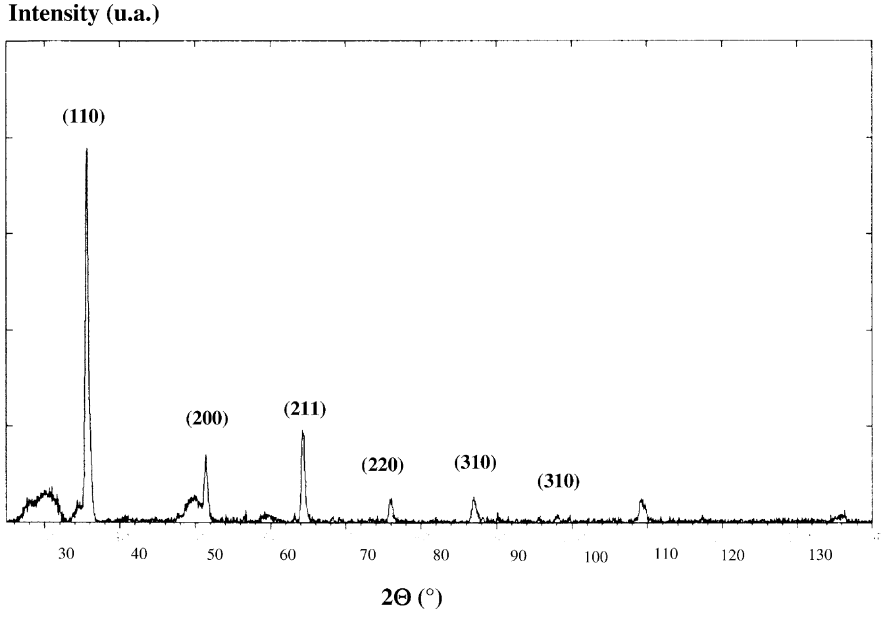

Fig. 2. X-ray diffraction spectrum obtained on an anodic dissolution residue showing typical diffraction peaks characteristic of the metastable β-Zr phase (Zr–1%Nb alloy after thermal treatment in the $\alpha + \beta$ temperature range)(alloy 6).

Table 3
Results from X-ray diffraction studies of residues obtained by electro-etching extraction performed on different Zr alloys allowing lattice parameter measurements

Alloy	Phase type	(h k l) considered to calculate the parameters	Parameters (nm)
1	$ZrFe_2$ ($P6_3/mmc$)	110; 103; 200; 112; 201; 004; 202; 213; 205; 220; 313	$a = 0.5031 \pm 0.0003$, $c = 0.8244 \pm 0.0008$
2	$ZrCr_2$ ($Fd\bar{3}m$)	220; 311; 222; 422; 511; 440; 533; 642; 731	$a = 0.7203 \pm 0.0003$
4	β-Zr ($Im3m$)	110; 200; 211; 220; 310; 321	$a = 0.3539 \pm 0.0003$
5	β-Nb ($Im3m$)	110; 200; 220; 310; 321	$a = 0.33294 \pm 0.00006$
6	β-Zr ($Im3m$)	110; 200; 211; 220; 310; 321	$a = 0.35377 \pm 0.00008$
10	$Zr_{60}Nb_{10}Fe_{30}$ ($Fm\bar{3}m$ or $F\bar{4}3m$)[a]	422; 333; 440	$a = 1.2309$
13	$Zr_{35}Nb_{35}Fe_{30}$ ($P6_3/mmc$)[a]	112; 201	$a = 0.5401$, $b = 0.8665$

[a] See [13] for discussion on the crystallographic spatial group of the ZrNbFe ternary intermetallic phases.

(or Mo) enriched β-Zr phase during cooling below the $T_{\alpha/\alpha+\beta}$ transus temperature. Then, long-term annealing treatments in the α phase temperature range are needed to achieve full equilibrium conditions [17], where the resultant equilibrium phase for Nb alloys is the β-Nb one.

Finally, we can notice that in alloy 9, the β-Zr phase corresponds to a 80Zr–15Nb–5Mo (at.%): niobium is partially substituted by molybdenum in this phase, both of them being β-stabilisers as previously discussed.

3.2. Crystallography of SPP

Anodic dissolution is an interesting way to isolate SPP from the surrounding matrix (α-Zr), which makes possible precise measurements of the lattice parameters

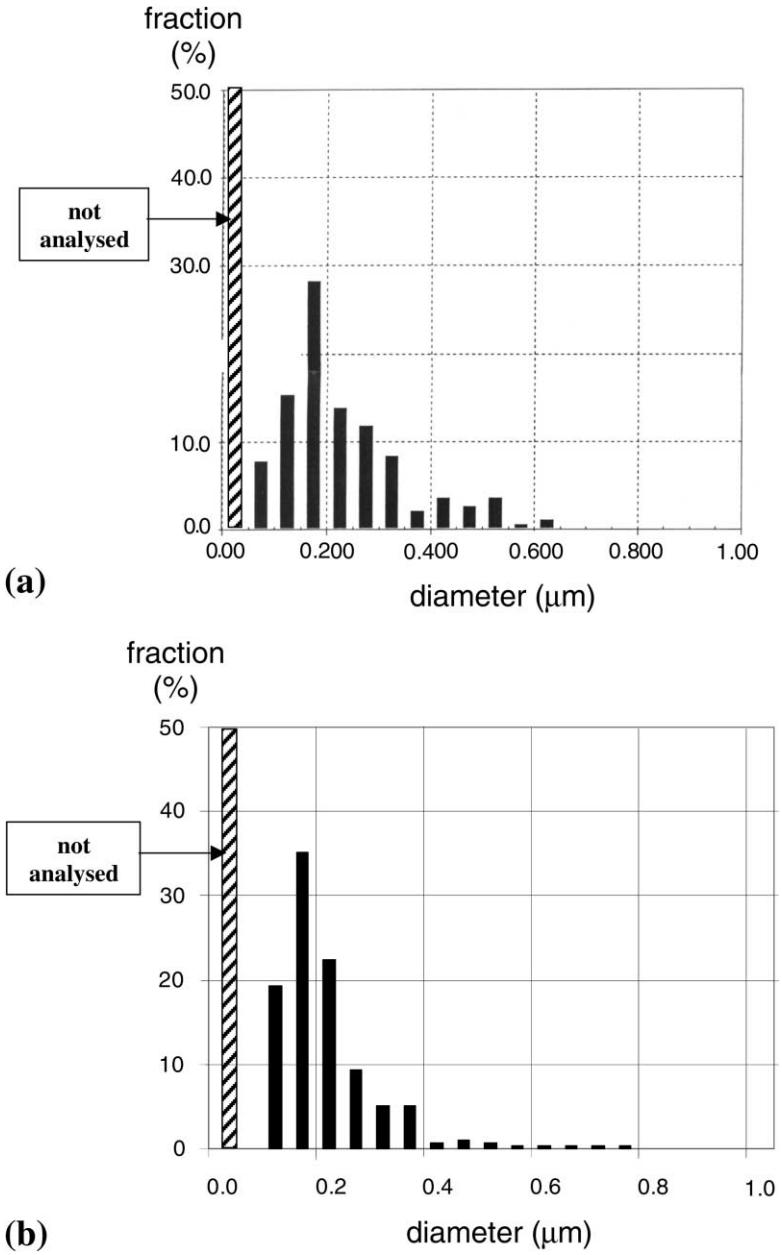

Fig. 3. Histograms of precipitate size distribution obtained by image analysing on a bulk Zy-4 (a) and an anodic dissolution residue extracted from the same alloy (b).

by X-ray diffraction. Fig. 2 shows an X-ray spectrum obtained on a residue extracted from a Zr–1%Nb alloy (alloy 6). Despite the presence of some matrix and zirconium oxide (ZrO_2) traces, the 2θ diffractogram of β-Zr can be correlated with the ASTM standard. The lattice parameter, calculated from 6 different crystallographic planes, is equal to $a = 0.3539 \pm 0.0003$ nm in this particular case.

The results obtained on different alloys are listed in Table 3. They confirm the stoichiometry of the main phases and give complementary data on the crystallographic structure (especially the lattice parameters).

To summarize, the phases observed (depending upon the thermal treatments applied) after anodic dissolution are:

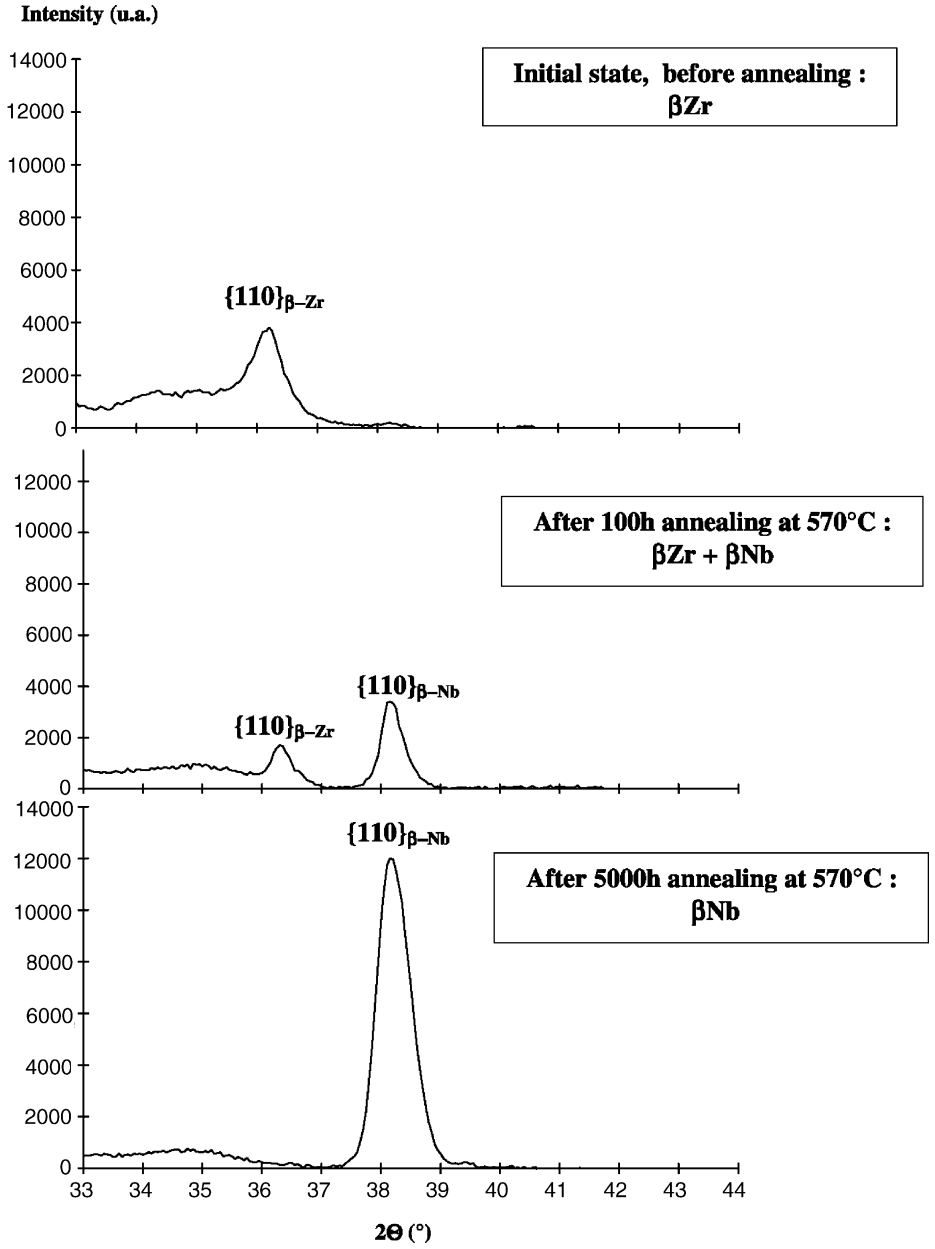

Fig. 4. X-ray diffraction spectrum obtained on an anodic dissolution residue showing the coexistence of the characteristic diffraction peaks of both β-Nb and β-Zr phases (Zr–1%Nb alloy after 100 h annealing at 570 °C).

- the metastable β-Zr phase enriched with Nb and/or Mo, formed at high temperature and retained at room temperature (alloys 4, 5 and 6),
- the stable phase of the $ZrFe_2$ type observed in Zr based alloys with high diffusion rate addition elements (alloy 1),
- the metastable phase of the $ZrCr_2$ type, observed in alloy 2,
- β-Nb observed in alloy 5 after long-term annealing treatments in the α domain,
- typical ternary intermetallic ZrNbFe phases observed in alloys 10 and 13.

3.3. Validation and application of anodic dissolution method

In order to validate the anodic dissolution procedure, we compared the SPP size distribution obtained by SEM observations combined with image analysis on, respectively, a bulk Zy-4 alloy and an anodic dissolution residue extracted from the same alloy. The results, presented in Fig. 3, show a very good agreement, and demonstrate that, for Zy-4, the SPP extracted by anodic dissolution are representative of the SPP present in the bulk, with no indication of selective extraction.

Also, this procedure was applied in order to follow the precipitation of β-Nb in a Zr–1%Nb alloy (containing initially β-Zr metastable precipitates) during long-term annealing treatments at 570 °C [17]. One must point out that, after having applied the dissolution procedure on different Zr–Nb alloys, we have never observed Nb redeposition as it can be observed with Sn on carbon replica for Zircaloys type alloys. In the literature, the mechanism of β-Nb precipitation, from an initial $\alpha +$ metastable β-Zr structure has not been studied in detail [18,19]. Thus, we have considered two possible extreme mechanisms:

(1) β-Nb phase occurrence by a progressive Nb enrichment of the metastable β-Zr phase, initially present in the alloy.
(2) Simultaneous dissolution of the metastable β-Zr phases and precipitation of the stable β-Nb ones.

One may notice that, using conventional TEM examinations, it is difficult to distinguish between these two mechanisms. Thus, we have studied the anodic dissolution residues by X-ray diffraction obtained after different annealing times at 570 °C. Indeed, the spectrum obtained on a sample annealed during 100 h clearly shows the coexistence of the characteristic peaks of both β-Nb and β-Zr phases (Fig. 4). Then, we were able to conclude that the mechanism of β-Nb precipitation was the second one.

4. Conclusion

In this study, carbon replica and an anodic dissolution procedures were used in order to determine stoichiometry and crystallographic parameters of different types of SPP, including metastable ones, in different types of zirconium alloys.

- Both procedures allowed us to extract and to determine precisely the stoichiometry and lattice parameters of all kinds of SPP observed in most Zr alloys, that is: β-Nb, β-Zr, Laves phase type intermetallic phases, ternary intermetallic phases: ZrNbFe.
- A quantitative validation of the anodic dissolution procedure was achieved for Zy-4 by comparing the size distributions of SPP obtained by extractions and directly measured on bulk Zy-4 alloy.
- This experimental procedure was also successfully applied to follow the precipitation of β-Nb phase at 570 °C in a Zr–1%Nb alloy containing initially β-Zr metastable precipitates [17].

Acknowledgements

The authors are grateful to P. Barberis and E. Cini (Framatome-ANP/Cezus) for some of the materials supplying and image analysis measurements on bulk Zy-4 (SPP size distribution). We also thank J.L. Béchade and T. Guilbert (CEA) for X-ray diffraction studies and P. Yvon and D. Gilbon (CEA) for editing the paper.

References

[1] R.J. Comstock, G. Schoenberger, G.P. Sabol, Zirconium in the Nuclear Industry: Eleventh Symposium, ASTM STP 1295, 1996, p. 710.
[2] V.N. Shishov, A.V. Nikulina, V.A. Markelov, M.M. Peregud, A.V. Kozlov, S.A. Averin, S.A. Kolbenkov, A.E. Novoselov, Zirconium in the Nuclear Industry: Eleventh Symposium, ASTM STP 1295, 1996, p. 603.
[3] B. Herb, H. Ruhmann, A. König, Zirconium in the Nuclear Industry: Twelfth Symposium, ASTM STP 1354, 2000, p. 482.
[4] S.A. Nikulin, V.I. Goncharov, V.A. Markelov, V.N. Shishov, Zirconium in the Nuclear Industry: eleventh symposium, ASTM STP 1295, 1996, p. 695.
[5] P. Barberis, E. Ahlberg, N. Simic, D. Charquet, M. Dahlbäck, M. Limbäck, P. Tägstsröm, C. Lemaignan, G. Wikmark, B. Lehtinen, Zirconium in the Nuclear Industry: Thirteenth Symposium, 10–14 June 2001, Annecy, France, ASTM STP 1423, in press.
[6] X. Yang, B. Zhou, Y. Jiang, C. Li, Nucl. Power Eng. 15 (1) (1994) 79.
[7] G. Jago, J.C. Brachet, O. Ast, J.L. Béchade, C. et Bataillon, Procédé de dissolution sélective de la matrice d'un alliage à

base de Zr et procédé d'analyse des phases précipitées ainsi extraites, Brevet Français no. 98 08146, 1998.
[8] V.N. Svechnikov, V.J. Markiv, V.V. Petkov, Metallofizika, Kiev, Akademiya Nauk Ukrainskoi SSR, Institut Metallofiziki, 42, 1972, p. 112.
[9] R.A. Versaci, M. Ipohorski, J. Nucl. Mater. 116 (1983) 321.
[10] H. Fujii, T. Okamoto, W.E. Wallace, F. Pourarian, T. Morisaki, J. Magnet. Magn. Mater. 46 (1985) 245.
[11] I.A. Popov, I.G. Rodionova, Russian, J. Inorg. Chem., translated from Zh. Neorgan. Khim. 9 (4) (1964) 489.
[12] D. Arias, T. Palacios, C. Turrillo, J. Nucl. Mater. 148 (1987) 227.
[13] C. Toffolon, J.C. Brachet, C. Servant, L. Legras, D. Charquet, P., Barberis, J.P. Mardon, Zirconium in the Nuclear Industry: Thirteenth International Symposium, 10–14 June 2001, Annecy, France, ASTM STP 1423, in press.
[14] A.V. Nikulina, V.N. Shishov, M.M. Peregud, A.V. Tselischev, V.K. Shamardin, C.P. Kobyliansky, J. Nucl. Mater. 238 (1996) 205.
[15] V.N. Shishov, M.M. Peregud, A.V. Nikulina, S.N. Akhromov, A.E. Novoselov, G.P. Kobylyansky, Z.E. Ostrovsky, V.K. Shamardin, Zirconium in the Nuclear Industry: Thirteenth International Symposium, 10–14 June 2001, Annecy, France, ASTM STP 1423, in press.
[16] V.V. Petkov, E.E. Cherkashin, Dopovidi Akademi Nauk Ukrains'koi Rsr, Seriya A, Fiziko-teknichni ta matematichni nauki 32 (3) (1972) 276.
[17] C. Toffolon, J.C. Brachet, T. Guilbert, D. Hamon, S. Urvoy, C. Servant, D. Charquet, L. Legras, J.P. Mardon, J. Phys. IV France 11 (2001) 99.
[18] P. Van Effenterre, G. Cizeron, P. Lacombe, J. Nucl. Mater. 31 (1969) 269.
[19] S.K. Menon, S. Banerjee, R. Krishnan, Metall. Trans. A 9A (1973) 1213.